AIP | Journal of Applied Physics

# Accessing intermediate ferroelectric switching regimes with time-resolved transmission electron microscopy

Christopher R. Winkler, Michael L. Jablonski, Anoop R. Damodaran, Karthik Jambunathan, Lane W. Martin et al.

Citation: J. Appl. Phys. **112**, 052013 (2012); doi: 10.1063/1.4746082
View online: http://dx.doi.org/10.1063/1.4746082
View Table of Contents: http://jap.aip.org/resource/1/JAPIAU/v112/i5
Published by the American Institute of Physics.

# Accessing intermediate ferroelectric switching regimes with time-resolved transmission electron microscopy

Christopher R. Winkler,[1] Michael L. Jablonski,[1] Anoop R. Damodaran,[2] Karthik Jambunathan,[2] Lane W. Martin,[2] and Mitra L. Taheri[1,a)]
[1]*Department of Materials Science & Engineering, Drexel University, Philadelphia, Pennsylvania 19104, USA*
[2]*Department of Materials Science & Engineering and Materials Research Laboratory, University of Illinois, Urbana-Champaign, Illinois 61820, USA*

(Received 1 March 2012; accepted 11 July 2012; published online 4 September 2012)

$BiFeO_3$ (BFO) is one of the most widely studied magneto-electric multiferroics. The magneto-electric coupling in $BiFeO_3$, which allows for the control of the ferroelectric and magnetic domain structures via applied electric fields, can be used to incorporate $BiFeO_3$ into novel spintronics devices and sensors. Before $BiFeO_3$ can be integrated into such devices, however, a better understanding of the dynamics of ferroelectric switching, particularly in the vicinity of extended defects, is needed. We use *in situ* transmission electron microscopy (TEM) to investigate the response of ferroelectric domains within $BiFeO_3$ thin films to applied electric fields at high temporal and spatial resolution. This technique is well suited to imaging the observed intermediate ferroelectric switching regimes, which occur on a time- and length-scale that are too fine to study via conventional scanning-probe techniques. Additionally, the spatial resolution of transmission electron microscopy allows for the direct study of the dynamics of domain nucleation and propagation in the presence of structural defects. In this article, we show how this high resolution technique captures transient ferroelectric structures forming during biasing, and how defects can both pin domains and act as a nucleation source. The observation of continuing domain coalescence over a range of times qualitatively agrees with the nucleation-limited-switching model proposed by Tagantsev *et al*. We demonstrate that our *in situ* transmission electron microscopy technique is well-suited to studying the dynamics of ferroelectric domains in $BiFeO_3$ and other ferroelectric materials. These biasing experiments provide a real-time view of the complex dynamics of domain switching and complement scanning-probe techniques. © *2012 American Institute of Physics*. [http://dx.doi.org/10.1063/1.4746082]

## I. INTRODUCTION

Ferroelectrics are a key class of materials for a variety of applications ranging from piezoelectric sensors and actuators, to non-volatile random-access memories, to solar energy conversion.[1–6] Recently, much research has focused on a subgroup of ferroelectrics that also possess magnetic properties (so-called multiferroic materials), which provide researchers with additional functional properties. Although there has been considerable attention given to multiferroism in materials, such as $BiFeO_3$ (BFO), it is a very rich and complex system and much remains to be learned about the fundamental nature of domain dynamics in this (and other multiferroic and ferroelectric) systems. In particular, it is important to better understand the factors that control and allow for the deterministic manipulation of ferroelectric switching and, in turn, magnetic order in such materials. Thus, the study of the temporal response of ferroelectric domains to external fields in multiferroics is vitally important for implementation of these materials into a range of applications. An improved understanding of the coupling processes under electric fields in these materials can help to predict and mitigate failures, which will aid in the development and optimization of future devices. This paper describes a method of *in situ* transmission electron microscopy (TEM) that reveals the fundamental processes associated with domain switching in multiferroic devices based on BFO at short temporal and spatial scales.

A ferroelectric domain can be defined as a region in which electric polarization is aligned along one of the energetically favored orientations, separated from other regions by domain walls.[7] Depending on the sample size (or thickness in thin films), domains can range from a few tens of nanometers in width to as large as the device itself.[8] The speed of domain wall motion is limited by the speed of sound in the material[9] and thus the dynamics of domain wall motion can range from picoseconds to milliseconds. Understanding this motion is crucial to the development of future devices. In general, domain switching begins when an electric field is applied and nuclei of switched polarization form at surfaces or on domain walls.[10] A general description of the domain switching process can be described in three key steps:[8,11] (a) reversed polarization nucleus formation, (b) growth of this nucleus parallel to the electric field direction, and then (c) lateral growth in the plane perpendicular to the electric field direction. Despite considerable work investigating domain switching in devices, limited dynamic imaging of this process has been completed. *In situ* techniques are ideally suited to investigating the validity of the different models of domain kinetics.

a)Author to whom correspondence should be addressed. Electronic mail: mtaheri@coe.drexel.edu.

 

The Kolmogorov-Avrami-Ishibashi (KAI) model is typically used to describe the kinetics of domain switching in both bulk and microscale ferroelectrics. The KAI model assumes the presence of random, independent nucleation sites from which, under an applied field, domains grow unhindered until the point of coalescence, whereupon these coalesced domains undergo lateral expansion as described in the third step above. As device geometries shrink into the nanoscale regime, it is found that the kinetics of ferroelectric switching in these smaller geometries can deviate from the KAI model.[12,13] Taganstev et al. have developed a new model, the nucleation-limited-switching (NLS) model, which better fits the switching kinetics of thin-film devices and nanoscale ferroelectric capacitors.[14] Briefly, the NLS model divides a ferroelectric device into separate regions, referred to as "elementary regions," and in each region independent domain nucleation can occur. An elementary region is considered switched when a domain of reverse polarization is nucleated within that region. As a consequence, the NLS model effectively treats ferroelectric switching as nucleation-limited, hence the name of the model. The fact that the ratio of nucleation sites – defects, domain walls, electrode interfaces – to nuclei per unit volume increases with shrinking device geometries may be one qualitative reason for the applicability of the NLS model over the KAI model in nanoscale systems. Thus, it is important to directly observe domain nucleation and propagation in real device systems as in this paper.

A myriad of techniques have been used to study domain switching behavior in ferroelectric materials.[15–27] One of the most notable techniques is piezoresponse force microscopy (PFM), which has given great insight into the nature of polarization switching in ferroelectric materials, including studies of nucleation at free surfaces[18] and in capacitor structures,[19] nucleation mechanisms, and domain wall dynamics.[20] Recent PFM experiments revealed the ability to directly observe domains in multiferroics and to control their switching behavior using electric fields.[16–20] Switching studies in PFM have focused mainly on imaging before and after switching and the details of the ferroelectric domain evolution during application of the field remains to be understood. This represents one of the limitations of PFM and other scanning-probe-based techniques in providing information on switching in these materials. Others limitations include (1) limited spatial resolution stemming from the fact that tip diameters are typically tens of nanometers in width, (2) slow scanning speed which makes direct measurement of kinetics difficult and renders probing processes at short time scales essentially impossible, and (3) near-surface sensitivity and information that arises from the fundamental nature of the scanning-probe process. It should be noted that recent advances in pulse train-based studies have improved the time resolution of scanned-probed-based studies,[28,29] but many uncertainties remain about intermediate processes that occur during switching, domain nucleation mechanisms and propagation kinetics, and domain-defect interaction, and this information is essential to better quantify domain dynamics in ferroelectric and multiferroic materials.

To overcome such limitations in temporal resolution when studying domain dynamics, researchers have used time-resolved photoemission electron microscopy (PEEM). In PEEM, excitation by polarized x-ray synchrotron radiation tuned to atomic absorption edges leads to the emission of secondary electrons at the sample surface, which are used to make an image of the sample.[30–33] It has been demonstrated that PEEM is capable of probing domain dynamics at nanosecond time resolution and sub-micron spatial resolution.[32,33] However, in general PEEM is unable to probe length scales less than 20–50 nm (Ref. 30) (although recent developments suggest that 10 nm spatial resolution is possible for some applications at the PEEM3 facility at the Advanced Light Source, Lawrence Berkeley National Laboratory[30]). Thus, the two most widely used techniques to probe domain switching have crucial limitations in spatial (PEEM and PFM) and temporal (PFM) resolution. It should be noted that scanning nonlinear dielectric microscopy (SNDM) is another probe-based technique which is sensitive to minute changes in the nonlinear dielectric constant induced by spontaneous polarization. The spatial resolution of the technique is comparable or better to that of PFM though the temporal resolution suffers because of the need to scan a probe as in PFM.[31]

At the same time, there have been remarkable advances in electron microscopy that have direct implications for the study of these materials, especially in the field of *in situ* TEM.[24–27,34] *In situ* TEM is a strong candidate to investigate domain switching phenomena over a critical spatial and temporal range. For the sake of comparison to the aforementioned techniques, Figure 1 maps the temporal and spatial resolution limits of PFM and PEEM, together with various contemporary *in situ* TEM techniques. The asterisk next to "PFM" denotes an acknowledgement that the use of pulse trains is currently being studied to improve temporal resolution of the technique.[28,29] It should also be noted that although Lorentz TEM and off-axis electron holography techniques[35–37] are useful tools for probing magnetization reversal in magnetic structures as a function of applied magnetic field, such techniques still have a number of major limitations. One issue is that the low-field objective lenses

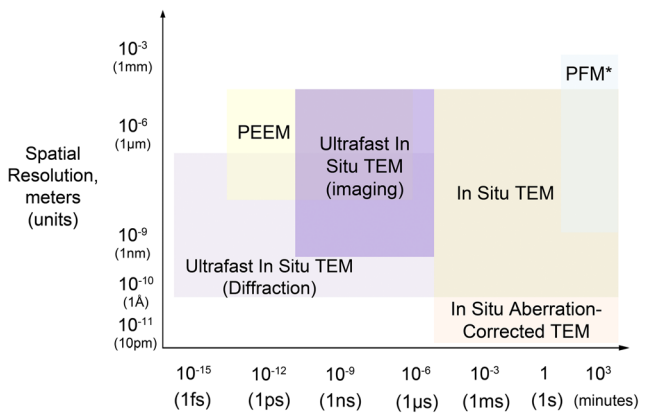


FIG. 1. Spatial and temporal resolution limits for techniques used to probe domain structures and dynamics. Note: this is not an all-inclusive list but compares methods discussed in this article. Asterisk denotes recent work on improving PFM spatial and temporal resolution.[38,39]

used for magnetic imaging have higher aberration coefficients than standard TEM lenses; thus, instead of a standard TEM's spatial resolution limit of less than 1 nm, the resolution limit in magnetic imaging is roughly 5–10 nm.[36] Using conventional lenses with *in situ* TEM has proven to be an effective method for understanding domain dynamics in ferroelectric materials,[24–27] however, and this is the focus of this paper.

Until the advent of *in situ* TEM, it had not been possible to directly observe the motion of domain walls, including wall velocity and shape change, with high spatial and temporal resolution. There has existed a gap between experiment and simulation due to a lack of techniques to probe fine details at high enough temporal resolution, while the computational cost of simulations that incorporate large enough cell sizes to perform grain scale studies on domain wall propagation are often prohibitively costly or must forgo inclusion of atomistic details.[10] A step toward closing this gap is taken in this work by using a dynamic electron microscopy technique that spans multiple time scales while maintaining high spatial resolution. Such resolution is needed to observe microstructural features, such as line defects. It has long been known that these defects directly impact ferroelectric response because they can interact with domain walls. For example, dislocations can block domain wall motion and they can also serve as sites for domain switching nucleation.[38–40] The results described in this paper present a foundation for developing a fundamental understanding of the ferroelectric domain evolution under electrical bias. This work employs an *in situ* TEM method that has advantages over the aforementioned techniques in that the ability to view intermediate stages will allow us to move forward in our understanding of the evolution of domains in this new class of materials.

Initial *in situ* biasing tests have demonstrated that the method presented herein for studying ferroelectric domain switching in multiferroic BFO structures is realistic for accessing domain dynamics with improved temporal and spatial resolution over traditional techniques. The results are comparable with those produced by PFM, yet the superior temporal resolution of this *in situ* technique permits study of the intermediate behaviors involved in ferroelastic switching. For example, our recent publication introducing these results[42] shows that we observed behavior that loosely follows the aforementioned three key steps of domain switching behavior: (1) the nucleation of a reversed polarization domain, (2) domain propagation parallel to the electric field direction, and (3) lateral domain growth perpendicular to the electric field direction. In this paper, we explore the use of this technique to study specific aspects of switching mechanisms with high temporal and spatial resolution. The ability to access intermediate steps in the switching process with this technique allows for comparison to theoretical models.

## II. EXPERIMENTAL

Domain switching behavior was observed using *in situ* TEM. The experiments were performed using a biasing holder (Hummingbird Scientific™, Lacey, WA) to probe the response of ferroelectric domains in BFO films and device structures. A DC bias was applied through a set of epitaxial in-plane electrodes, thereby enabling control of ferroelectric switching in the sample. Domain wall nucleation and movement were captured using digital streaming video at 30 Hz (0.033 s time resolution), at both low and high magnifications, and this information will be analyzed to measure domain kinetics and nucleation energies.

$BiFeO_3$(BFO)/$SrRuO_3$(SRO)/$SrTiO_3$(STO) (001) heterostructures were prepared using pulsed-laser deposition. Because of the geometric limitations of the TEM, the structures to be studied by *in situ* TEM were engineered to emulate cross-sectional capacitor structures common to device applications. Specifically, the samples were prepared by growing an epitaxial layer of the electrode material SRO (generally 25–100 nm), followed by a lithography and precision ion-milling step to define the complex planar-electrode structure (Figure 2(a)). A second growth run produced an epitaxial layer of BFO on top of the device structure which is omitted from Figure 2 for clarity. The structures consisted of 35–100 nm thick BFO films grown on substrates of STO (001) with planar SRO electrodes, permitting the application of in-plane electric fields. The distance between the SRO electrodes in this study is ~4 $\mu$m but can be varied during the lithography process. Samples were grown such that the ferroelectric polarization of the BFO film is downward (towards the substrate) pointing, reducing the number of unique polarization vectors from eight to four (Figure 2(b)). The number of unique ferroelastic domains remains four in this configuration.

The imaging under electrical biasing was performed in a plan-view geometry as illustrated in Figure 2. The field of view during the TEM experiments was concentrated within the two "trenches" milled between the SRO electrodes (Figure 2(c)). In order to have a uniform electric field, the samples are thinned uniformly using a focused ion beam (FIB), ensuring a flat surface of BFO between the SRO planar electrodes. To

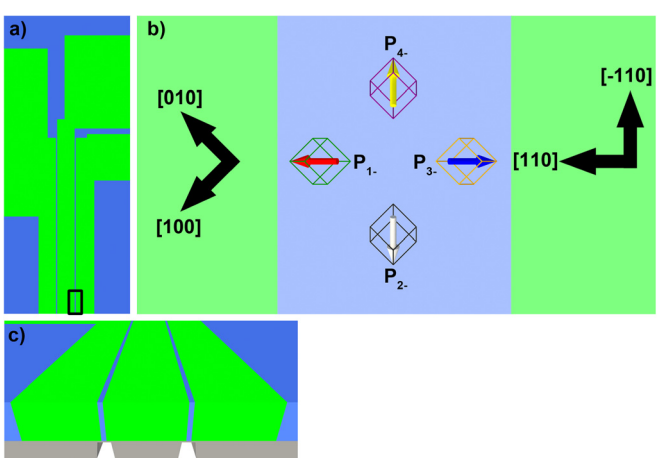


FIG. 2. BFO device geometry for *in situ* biasing. (a) Plan view of device looking down the [001] direction showing the patterned SRO electrodes (green) and BFO trenches between them (blue). (b) A magnified view of the boxed region in (a) which illustrates the direction of the applied electric field, principal crystallographic directions, and the projection of the ferroelectric (arrows) and ferroelastic (rhombi) domains in the BFO trench. (c) Isometric front view of same BFO device. Samples are tripod polished to remove most of the bulk STO and then electron transparent channels are milled underneath the BFO trenches using FIB.

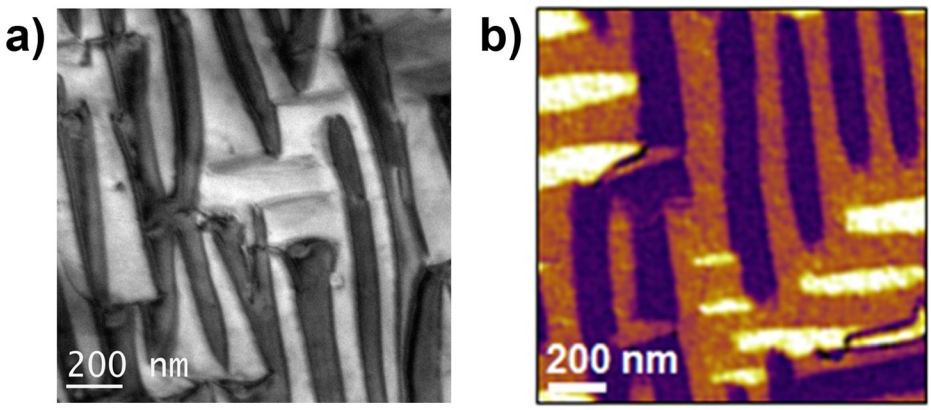


FIG. 3. Comparison of a BF TEM images (a) and an in-plane phase PFM image (b), revealing the ability of TEM to probe domains.

ensure that the configuration of the sample was controlled, the samples are prepared using a combination of tripod polishing and FIB milling techniques. Care was taken during FIB milling to ensure minimal sample damage (it should be noted that the FIB milling occurred from the back (substrate side) of the sample which minimized damage to the BFO layer). During TEM experiments, the samples were biased, and simultaneously imaged using digital streaming video.

Our experimental setup is advantageous because it enables real-time monitoring of an entire device structure during *in situ* operation, and because ferroelectric switching is accomplished via the use of in-plane electrodes. In-plane electrodes eliminate the sample surface-probe tip barrier present in experiments using scanning probes to initiate ferroelectric switching. This eliminates ambiguities associated with tip shapes and non-linear electric fields away from the tip center. Additionally, in-plane electrodes eliminate the out-of-plane depolarizing fields generated at the film and bottom conductive layer interface. These depolarizing fields introduce an internal bias which strongly affects switching behavior, and such internal fields can be difficult to quantify. The large field of view permits the simultaneous observation of all ferroelectric domains within the volume of a device, and the real-time interaction of domains with other domains, nuclei and dislocations under bias. For the studies reported here, voltages between 45 and 100 V were applied between the electrodes, resulting in applied electric field strengths of approximately 115 and 250 kV cm$^{-1}$. The results of a few key biasing experiments are discussed in Sec. III.

## III. RESULTS AND DISCUSSION

To test the feasibility of repeated switching experiments in the TEM, static bright field images were first taken to determine the ability to see domains. A comparison is shown in Figure 3, where Fig. 3(a) is a TEM image of the domains already examined by PFM (Fig. 3(b)). Figures 3(a) and 3(b) both show stripe-like domains containing four ferroelectric variants, which represent the domain configuration that was studied in this work. These stripe domains are primarily separated by so-called 71° domain walls, which lie on {101} planes.[41] The domain walls are thus inclined 45° with respect to the [001] zone axis.

Processes such as heterogeneous domain nucleation from existing domain walls, relaxation behavior of individual domains, and defect-domain interactions were observed during *in situ* biasing experiments. These events are clearly seen in Figure 4, which reveals the ability to view domain switching and defect-domain interactions in BFO, which is not possible with other characterization methods. The image sequence in Figure 4 highlights intermediate stage events, such as domain wall collisions (Fig. 4(b), right-hand side of Fig. 4(c), and the domains highlighted in purple and yellow in Figs. 4(e) and 4(f)), domain wall-dislocation interactions (Fig. 4(b), at the dislocation network on left of Fig. 4(c), and in the domains nucleating on dislocations highlighted in red in Figs. 4(c) and 4(f)), nucleation (Fig. 4(b), the domains nucleating at the top middle as well as on the dislocation network in Fig. 4(c), and the nuclei highlighted in red in

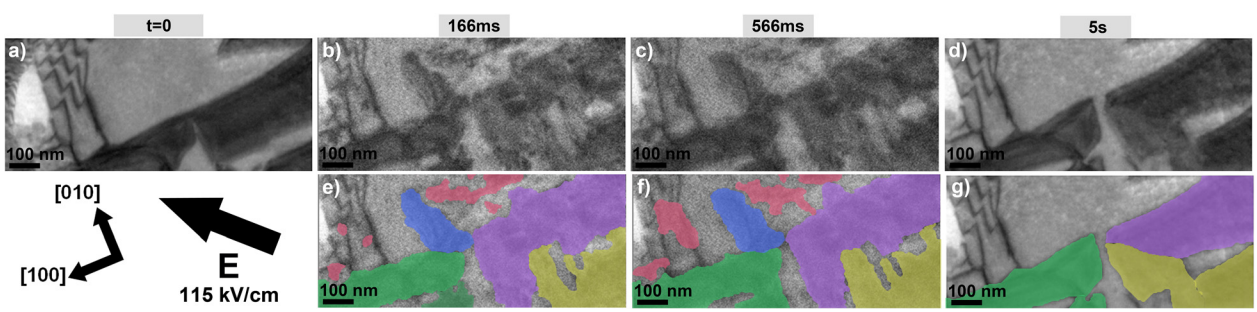


FIG. 4. A sequence of bright field TEM images taken during *in situ* biasing of a BFO device structure at +45 V (115 kV/cm). Crystallographic and electric field directions are indicated lower left. "Pre" and "Post," indicated as t = 0 and t = 5 s, denote the domain morphology before the field was applied and 5 s after the field was turned off, respectively. Images from 166 ms (b) and 566 ms (c) are selected frames extracted from the *in situ* video. Images (e)-(g) contain colored overlays (color online) to guide the eye in viewing the many changes in domain morphology during switching events.

Figs. 4(e) and 4(f)), relaxation (Figs. 4(d) and 4(g) and also note the absence of the nucleated and propagated domains in Figs. 4(b) and 4(c)) that had not yet been observed or imaged by other methods. These results confirm that *in situ* TEM methods are useful for studying domain switching events and quantifying kinetic behavior as a function of microstructural features, such as dislocations, point defect clusters, and other domain walls. The way in which this behavior affects critical events, such as domain relaxation, is explored in great detail in Ref. 40.

There is clear evidence of domains nucleating on the dislocation network formed at the junction between the electrode and the BFO trench in Figure 4. However, the same figure also shows domains nucleating in an area with no visible extended defects. In light of the non-cooperative domain behavior seen in Figure 4, one can infer that domain wall-defect interactions beyond those directly visible are taking place. Specifically, domains may be nucleating at point defect clusters in the local vicinity. These initial experiments demonstrate the ability to see microstructural features (e.g., line defects) beyond domain walls is possible using *in situ* TEM. Despite the inability to see individual point defects, the imaging capabilities shown here provide a foundation for studies involving strain fields from any line defects that are present in the sample.

The newly nucleated domains shown in Figures 4(b) and 4(c) are grouped and divided into four different regions, as shown in Figure 5(a). Region I is comprised of three individual nuclei, highlighted with blue overlay, which form on the electrode edge and within a network of dislocations present within that film-electrode interface. Region II also contains three nuclei, red overlay, though the largest element appears to be a cluster of coalesced nuclei. Region III includes two domains, green overlay, one of which is a small nucleus and the other a larger domain which nucleated and propagated off the domain wall of the nearby preexisting domain. Region IV is composed of a single, large domain, purple overlay, which has also nucleated and propagated off a pre-existing domain wall. The projected domain area for each of the individual domains in all four regions was calculated using an edge finding algorithm to identify domain boundaries. Domain areas were calculated for each frame for which the voltage pulse is applied in the acquired *in situ* video. A plot of domain areas versus time, grouped by region, is shown in Figure 5(b).

This plot reveals a few clear trends: First, all four regions experience a collective increase in domain area versus time for the first 300 ms of the applied voltage pulse. After this period, competition between neighboring domain regions, namely, domain region II versus regions III and IV, prohibits domains in region II from expanding further, and even causes domain contraction. Essentially, domains in region II are pinned between the expanding domains in regions III and IV. The nature of this competition is apparently dominated by electrostatic effects, as the domains can be seen to actively repulse one another when driven into interaction by the applied field. One explanation of this repulsion is that it is driven by the formation of head-to-head and tail-to-tail domain walls configurations between the various nucleated and propagated domains. These charged domain walls are temporarily supported by the applied electric field and the removal of the field corresponds with the collapse of these transient domain structures. Despite the inter-region repulsive effects, some domains within a specified region are observed coalescing in the intermediate video frames. Domain areas in Region I are not limited in their expansion like those of the other three regions and are observed to continuously grow and expand versus time. This

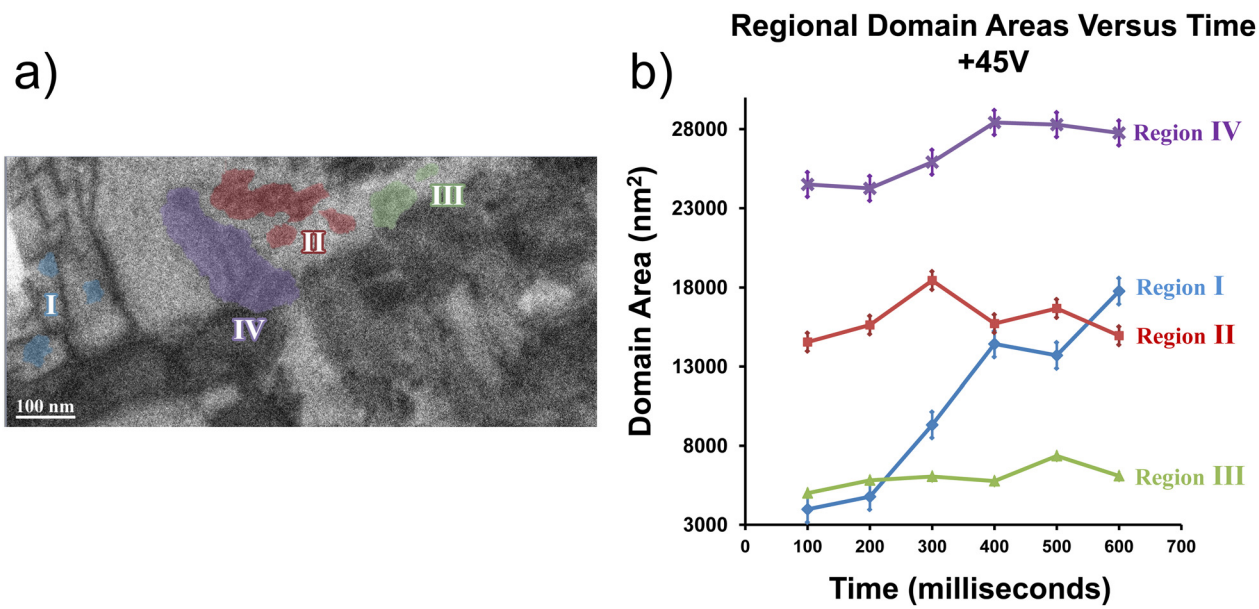


FIG. 5. Domains shown in Figure 4 are grouped into four different regions (a) and the cumulative domain areas in each of the four regions versus time are plotted (b). Region I is comprised of domains (blue highlight) nucleating at the electrode edge and along the network of existing dislocations. Region II includes a larger cluster of nuclei and two smaller, individual nuclei (red highlight). Region III consists of one small nuclei and one larger domain (green highlight). The larger domain in region III has nucleated and propagated off an existing domain wall. Region IV is composed of a single, large domain which has also nucleated and propagated from an already present domain wall (purple highlight).

growth is likely due to the effects of the dislocation network, which can lower the local coercive field of the BFO film, and domain coalescence which is visible in Figures 4(c) and 4(f). Two of the three domains in this region coalesce into one larger domain, and it appears that each domain is pinned by a nearby dislocation, behavior which is consistent with theory.

The intermediate processes observed by this experimental technique qualitatively agree with the NLS model. Upon application of an electric field, many different nuclei are observed through the volume of the film. While these nucleation events occur on orders of magnitude smaller time scales than the temporal resolution of this *in situ* technique, the observed morphologies of these nuclei are indicative of their evolution. For example, while some of the nuclei are small and circular (in projection), for example, the domains in region I, and the two smaller domains in region II, the large domain in region II is clearly composed of many different nuclei that have coalesced into a single domain. During the duration of the applied pulse, further coalescence of nuclei is observed. The evolving coalescence is consistent with the broad ferroelectric switching times distribution suggested by the NLS model. Repulsion and other interactions prohibit any single reversed polarity domain from unrestrictedly expanding throughout the volume of the region observed, though certain types of intrinsic defects can act as nucleation sites. While the experimental evidence suggests the treatment of ferroelectric thin-film devices as ensemble regions, each exhibiting a broad range of switching times, further experimental work over different time scales and ranges is necessary to confirm the NLS model of ferroelectric switching in thin films. It is clear that while our early results presented in this paper favor neither model perfectly, the experimental technique we use serves as an excellent means of validating models of ferroelectric domain switching and will aid in future predictive materials development in the area of ferroelectric device applications.

The experiments presented in this paper are challenging on many fronts. One major area of difficulty is sample preparation. We have observed that FIB-only preparation could leave a large amorphous layer on the surface of the sample, preventing ultra-high resolution imaging. Using low accelerating voltage milling in the FIB and post-FIB low energy argon ion milling can minimize the thickness of this amorphous layer. A second challenge to be addressed in this work is the development of improved voltage control for *in situ* studies. As is common with any electrical biasing study of ferroelectrics, the infinite voltage ramp rate and lag-time have been shown to provide confusion and make it difficult to correlate distinct aspects of the nucleation and switching mechanism in the most optimal time-resolved manner. Improved electronics can alleviate this issue for future experiments. An improvement in the imaging speed of TEM cameras would be a major boon to these experiments, as well as to the entire field of *in situ* electron microscopy. An increase in temporal resolution brought on by faster than TV rate cameras would allow for improved imaging of domain propagation and help bridge the time resolution gap between standard *in situ* TEMs and other ultrafast techniques, such as the dynamic TEM (DTEM) technique, which is able to access nanosecond time scales with nanometer spatial resolution.[41,43–47]

## IV. CONCLUSIONS

A need exists to advance our fundamental understanding of the mechanisms by which defects, surfaces, and interfaces influence the properties and behavior of materials, including ferroelectrics and multiferroics. This need challenges us to develop an understanding of the surfaces and interfaces in magnetoelectrically coupled device architectures in electric fields. Meeting this challenge will require a quantitative multiscale approach that addresses microstructure dependence of electrically driven processes and will provide a foundation for predictive materials development. This paper presents a significant leap toward the development of a fundamental understanding of the microstructural mechanisms in electric field control of ferroelectric and multiferroic materials. This information can be compared to molecular dynamics and stochastic models to test and enhance accepted theories of nucleation and growth and enables us to understand how the presence of defects and localized compositional changes play a role in domain wall motion behavior during electric field control of future devices. The techniques and instrumentation presented in this paper can be extended to investigate the nanoscale properties of other important classes of materials, such as piezoelectrics, pyroelectrics, and ferroelastics.

## ACKNOWLEDGMENTS

M.L.T, C.R.W., and M.L.J. gratefully acknowledge support from the National Science Foundation under Grant No. CMMI-1031403 as well as from the Office of Naval Research under Grant No. N00014-1101-0296. C.R.W. acknowledges support from the United States Department of Education and Drexel University through the GAANN-DREAM fellowship under Contract No. P200A060117. K.J. and L.W.M. acknowledge support from the Office of Naval Research under Grant No. N00014-10-10525. A.R.D. and L.W.M. acknowledge support from the Army Research Office under Grant No. W911NF-10-1-0482. Experiments at UIUC were carried out in part in the Frederick Seitz Materials Research Laboratory Central Facilities. Electron microscopy experiments were conducted in Drexel University's Centralized Research Facilities.

[1]M. Bibes and A. Barthélémy, Nature Mater. **7**, 425 (2008).
[2]D. Lee, S. M. Yang, T. H. Kim, B. C. Jeon, Y. S. Kim, J. G. Yoon, H. N. Lee, S. H. Baek, C. B. Eom, and T. W. Noh, Adv. Mater. **24**, 402 (2012).
[3]K. Takanashi, N. Kida, and M. Tonouchi, Phys. Rev. Lett. **96**, 117402 (2006).
[4]H. Bea, M. Gajek, M. Bibes, and A. Barthélémy, J. Phys.: Condens. Matter **20**, 434231 (2008).
[5]S. Y. Yang, J. Seidel, S. J. Byrnes, P. Shafer, C. H. Yang, M. D. Rossell, P. Yu, Y. H. Chu, J. F. Scott, J. W. Ager, L. W. Martin, and R. Ramesh, Nat. Nanotechnol. **5**, 143 (2010).
[6]S. R. Basu, L. W. Martin, Y. H. Chu, M. Gajek, R. Ramesh, R. C. Rai, X. Xu, and J. L. Musfeldt, Appl. Phys. Lett. **92**, 091905 (2008).
[7]Y. H. Chu, L. W. Martin, M. B. Holcomb, M. Gajek, S. J. Han, Q. He, N. Balke, C. H. Yang, D. Lee, W. Hu, Q. Zhan, P. L. Yang, A. Fraile-Rodgriguez, A. Scholl, S. X. Wang, and R. Ramesh, Nature Mater. **7**(6), 478 (2008).
[8]A. Gruverman and A. Kholkin, Rep. Prog. Phys. **69**(8), 2443 (2006).

[9]M. Dawber, K. M. Rabe, and J. F. Scott, Rev. Mod. Phys. **77**, 1083–1130 (2005).
[10]P. Paruch, T. Giamarchi, and J. M. Triscone, Phys. Rev. Lett. **94**, 197601 (2005).
[11]S. Jesse, B. J. Rodriguez, S. Choudhury, A. P. Baddorf, I. Vrejoiu, D. Hesse, M. Alexe, E. A. Aliseev, A. N. Morozovska, J. Zhang, L. Q. Chen, and S. V. Kalinin, Nature Mater. **7**(3), 209 (2008).
[12]Y. Kim, H. Han, W. Lee, S. Baik, D. Hesse, and M. Alexe, Nano Lett. **10**, 1266 (2010).
[13]D. Pantel, Y.-H. Chu, L. W. Martin, R. Ramesh, D. Hesse, and M. Alexe, J. Appl. Phys. **107**, 084111 (2010).
[14]A. Tagantsev, I. Stolichnov, N. Setter, J. Cross, and M. Tsukada, Phys. Rev. B **66**, 214109 (2002).
[15]N. Balke, I. Bdikin, S. V. Kalinin, and A. L. Kholkin, J. Am. Ceram. Soc. **92**, 1629–1647 (2009).
[16]Y.-H. Chu, L. W. Martin, M. B. Holcomb, M. Gajek, S.-J. Han, Q. He, N. Balke, C.-H. Yang, D. Lee, W. Hu, Q. Zhan, P.-L. Yang, A. Fraile-Rodríguez, A. Scholl, S. X. Wang, and R. Ramesh, Nature Mater. **7**, 478–482 (2008).
[17]Y.-C. Chen, G.-F. Wang, H.-H. Tai, J.-W. Chen, Y.-C. Huang, J.-C. Yang, and Y.-H. Chu, Nanotechnology **22**, 254030 (2011).
[18]A. Gruverman, B. J. Rodriguez, C. Dehoff, J. D. Waldrep, A. I. Kingon, R. J. Nemanich, and J. S. Cross, Appl. Phys. Lett. **87**, 082902 (2005).
[19]D. J. Kim, J. Y. Jo, T. H. Kim, S. M. Yang, B. Chen, Y. S. Kim, and T. W. Noh, Appl. Phys. Lett. **91**, 132903 (2007).
[20]S. V. Kalinin, B. J. Rodriguez, A. Y. Borisevich, A. P. Baddorf, N. Balke, H. J. Chang, L.-Q. Chen, S. Choudhury, S. Jesse, P. Maksymovych, M. P. Nikiforov, and S. J. Pennycook, Adv. Mater. **22**, 314–322 (2010).
[21]S. O. Hruszkewycz, C. M. Folkman, M. J. Highland, M. V. Holt, S. H. Baek, S. K. Streiffer, P. Baldo, C. B. Eom, and P. H. Fuoss, Appl. Phys. Lett. **99**, 232903 (2011).
[22]D.-H. Do, P. G. Evans, E. D. Isaacs, D. M. Kim, C. B. Eom, and E. M. Dufresne, Nature Mater. **3**, 365–369 (2004).
[23]D. Lebeugle, A. Mougin, M. Viret, D. Colson, and L. Ranno, Phys. Rev. Lett. **103**, 257601 (2009).
[24]C. T. Nelson, P. Gao, J. R. Jokisaari, C. Heikes, C. Adamo, A. Melville, S.-H. Baek, C. M. Folkman, B. Winchester, Y. Gu, Y. Liu, K. Zhang, E. Wang, J. Li, L.-Q. Chen, C.-B. Eom, D. G. Schlom, and X. Pan, Science **334**, 968–971 (2011).
[25]H. Chang, S. V. Kalinin, S. Yang, P. Yu, S. Bhattacharya, P. P. Wu, N. Balke, S. Jesse, L. Q. Chen, R. Ramesh, S. J. Pennycook, and A. Y. Borisevich, J. Appl. Phys. **110**, 052014 (2011).
[26]X. Tan, Z. Xu, and J. K. Shang, Mater. Sci. Eng., A **314**, 1–2 (2001).
[27]H. He and X. Tan, Phys. Rev. B **72**, 024102 (2005).
[28]N. A. Polomoff, A. Rakin, S. Lee, V. Palumbo, P. Yu, Y. H. Chu, R. Ramesh, and B. D. Huey, J. Appl. Phys. **109**, 091607 (2011).
[29]N. A. Polomoff, R. N. Premnath, J. L. Bosse, and B. D. Huey, J. Mater. Sci. **44**, 19 (2009).
[30]A. Scholl, Curr. Opin. Solid State Mater. **7**, 59–66 (2003).
[31]Y. Cho, S. Kazuta, and K. Matsuura, Appl. Phys. Lett. **75**, 2833 (1999).
[32]J. Vogel, W. Kuch, M. Bonfim, J. Camarero, Y. Pennec, F. Offi, K. Fukumoto, J. Kirschner, A. Fontaine, and S. Pizzini, Appl. Phys. Lett. **82**, 2299 (2003).
[33]T. Zhao, A. Scholl, F. Zavaliche, K. Lee, M. Barry, A. Doran, M. P. Cruz, Y. H. Chu, C. Ederer, N. A. Spaldin, R. R. Das, D. M. Kim, S. H. Baek, C. B. Eom, and R. Ramesh, Nature Mater. **5**, 823–829 (2006).
[34]S. P. Venkateswaran, N. T. Nuhfer, and M. De Graef, Acta Mater. **55**, 16 (2007).
[35]M. Tanase and A. K. Petford-Long, Microsc. Res. Tech. **72**(3), 187 (2009).
[36]K. He, D. J. Smith, and M. R. McCartney, Appl. Phys. Lett. **95**, 182507 (2009).
[37]C. Phatak, M. Beleggia, and M. De Graef, Ultramicroscopy **108**(6), 503 (2008).
[38]P. Maksymovych, J. Seidel, Y. H. Chu, P. Wu, A. P. Baddorf, L.-Q. Chen, S.V. Kalinin, and R. Ramesh, Nano Lett. **11**, 1906 (2011).
[39]S. P. Alpay, I. B. Misirlioglu, V. Nagarajan, and R. Ramesh, Appl. Phys. Lett. **85**, 2044 (2004).
[40]C. R. Winkler, A. R. Damodaran, J. Karthik, L. W. Martin, and M. L. Taheri, Micron **43**, 1121 (2012).
[41]M. L. Winkler, B. W. Reed, T. B. LaGrange, and N. D. Browning, Small **4**, 12 (2008).
[42]C. R. Winkler, M. L. Jablonski, A. R. Damodaran, J. Karthik, J. G. Wen, D. J. Miller, L. W. Martin, and M. L. Taheri, "Ferroelectric switching dependence on defect-domain wall interactions in $BiFeO_3$," (unpublished).
[43]M. L. Taheri, T. LaGrange, B. W. Reed, M. R. Armstrong, G. H. Campbell, W. J. DeHope, J. S. Kim, W. E. King, D. J. Masiel, and N. D. Browning, Microsc. Res. Tech. **72**(3), 122 (2009).
[44]J. S. Kim, T. Lagrange, B. W. Reed, M. L. Taheri, M. R. Armstrong, W. E. King, N. D. Browning, and G. H. Campbell, Science **321**, 5895 (2008).
[45]T. Lagrange, G. H. Campbell, B. W. Reed, M. Taheri, J. Pesavento, J. Kim, and N. Browning, Ultramicroscopy **108**, 11 (2008).
[46]M. L. Taheri, S. McGowan, L. Nikolova, J. E. Evans, N. Teslich, J. P. Lu, T. LaGrange, F. Rosei, B. J. Siwick, and N. D. Browning, Appl. Phys. Lett. **97**, 032102 (2010).
[47]I. M. Robertson, C. A. Schuh, J. S. Vetrano, N. D. Browning, D. P. Field, D. J. Jensen, M. K. Miller, I. Baker, D. C. Dunand, R. Dunin-Borkowski, B. Kabius, T. Kelly, S. Lozano-Perez, A. Misra, G. S. Rohrer, A. D. Rollett, M. L. Taheri, G. B. Thompson, M. Uchic, X. L. Wang, and G. Was, J. Mater. Res. **26**, 11 (2011).